

Influence of different fluoride containing electrolytes on the formation of self-organized titania nanotubes by Ti anodization

J. M. Macak · L. V. Taveira · H. Tsuchiya · K. Sirotna ·
J. Macak · P. Schmuki

Received: June 2, 2005 / Revised: July 15, 2005 / Accepted: July 29, 2005
© Springer Science + Business Media, Inc. 2006

Abstract The formation of self-organized porous titania nanotubes is achieved by electrochemical anodization under specific experimental conditions. In present work, the formation of porous titania nanotubes on titanium substrates is investigated in several $\text{SO}_4^{2-}/\text{F}^-$ based electrolytes. The presence of some non-porous layers covering the porous layers and accompanying the pore growth is observed. We discuss in details the influence of different electrolyte composition on the structure of self-organized porous layers, investigate the conditions for ideal pore growth. SEM investigations and XRD, AES and EDX surface analyses are carried out to characterize the self-organized porous layers. The results show that using $\text{SO}_4^{2-}/\text{F}^-$ electrolytes with different cations can drastically influence the final morphology of the self-organized porous nanotubes. We furthermore show that the nanotubes consist of TiO_2 and that they remain unchanged when annealed.

Keywords Self-organization · Titanium dioxide · Nanotube · Oxide dissolution

Introduction

Self-organized nanostructures such as ordered porous alumina [1, 2], macroporous silicon [3, 4] or InP [5] have re-

ceived considerable attention due to the anticipated high technological potential, which arises from huge aspect ratio and semiconductor properties. For instance porous alumina substrates are widely used as a template [6], due to optical properties they may serve as photonic crystals or waveguides [7, 8]. Typically, the conditions for the electrochemical formation of self-organized nanostructures are very defined, e.g. specific applied anodic potential, electrolyte composition and temperature are the most important parameters for formation of self-organized porous alumina.

Also the anodization of titanium has been studied for many decades in a wide range of electrolytes, but only a short time ago nanoporous titania by electrochemical means has been discovered [9]. Recently a few novel methods for a structuring of titanium on the nanoscale (10 nm–range) have been investigated such as sol-gel methods [10], metallorganic chemical vapor deposition (MOCVD) [11] or templating [12]. On the other hand, the formation of microporous and crystalline TiO_2 , which can be profitably used due to its bioactivity as the interface between Ti implants and bones [13], by electrochemical anodization under high voltages (so-called sparking anodization) has been investigated by several researches [14, 15]. Another method, which was developed quite recently by several research groups [16, 17], is based on electrochemical anodization in acidic electrolytes containing small amounts of hydrofluoric acid (HF), which leads to a formation of self-organized nanoporous titania. It was shown in our previous work [17] that the porosification process in HF electrolytes is essentially based on a competition between the pore formation at the inner (metal-oxide) interface and a chemical dissolution of the oxide at the outer interface (oxide-electrolyte). However as a result of the high dissolution rate of TiO_2 in HF electrolytes only a limiting thickness of the porous titania can be achieved (~ 500 nm). TiO_2 is attacked in fluoride media under the formation of a highly soluble $[\text{TiF}_6]^{2-}$ complex.

J. M. Macak · L. V. Taveira · H. Tsuchiya · P. Schmuki (✉)
University of Erlangen-Nuremberg, Department of Materials
Science, Chair for Surface Science and Corrosion, D-91058
Erlangen, Germany
e-mail: schmuki@ww.uni-erlangen.de

K. Sirotna · J. Macak
Institut of Chemical Technology Prague, Department of Power
Engineering, CZ-16628 Prague, Czech Republic

This dissolution of titania is required for the pore formation, but on the other hand avoids the thickening of the porous layer, because when the pH is low the dissolution rate is too high (as shown in our recent publications [18, 19]).

Very recently we obtained for the first time high-aspect ratio self-organized nanotubular titania layers with thickness higher than $2\text{ }\mu\text{m}$ by tailored anodization in neutral electrolytes containing NH_4F instead of HF [19, 20]. Thereby we exploit the slower chemical etching of titania because for elevated pH and the fact that the hydrolysis reaction at the pore tip produces an acidic environment by adjusting the dissolution current and thereby the pH—profile along the TiO_2 nanotubes, in a manner that local acidification occurs at the pore tip while the pH-values established at the pore mouths are higher due to the buffer species $(\text{NH}_4)_2\text{SO}_4/\text{NH}_4\text{F}$ [19]. Some other groups confirmed the findings in various electrolytes [21–24]. Common to all previous works [16–24] is that self-organization processes require time and depend on a wide range of the electrochemical parameters. The self-organized nanotube titania layers feature a good mechanical strength, wear resistance and chemical stability and bears a huge potential in view of its applications. Titanium dioxide is well known for self-cleaning properties due to the ability to photocatalytically degrade organic molecules [25], due to high gas sensitivity as a gas sensor [26]. For its high bioactivity is widely used in medicine as a cover of dental or bone titanium implants [13, 27].

Additionally, we have recently formed self-organized porous structures as well on biomedical Ti-alloys [28] and on a whole range of other valve metals such as Zr [29, 30], Hf [31], W [32], Ta [33, 34], Nb [35] under optimized electrochemical conditions. These nanoarchitected oxide films have very specific functional properties compared to their substrates, which are applicable in optics, electronics, photochemistry and biology. For example porous zirconia (ZrO_2) is promising biocompatible material [36] and together with porous hafnia [31] bears an enormous technological potential due to the extremely high-aspect ratio (more than 100) coming from the length of nanotubes in a range of dozens of μm [37].

The present study investigates the possibility to achieve self-organized porous titania layers in neutral sulphate electrolytes with small additions of fluorides (both the anions coupled in all cases with the identical cations—ammonium, cesium, potassium or sodium) and compares their influence in view of final resolution, i.e. pore morphology and thickness of nanoporous oxide films grown on titanium. We investigate also the influence of a thermal annealing on the pore structure and morphology. The formed layers are characterized with SEM, XRD, XPS and EDX. This with the aim of an expansion of earlier work in view of understanding the effects of the electrolyte composition on the pore formation.

Experimental

Titanium sheets (0.1 mm, 99.6% purity, Goodfellow, England) were firstly degreased by sonicating in acetone, isopropanol and methanol, afterwards rinsed with deionized (DI) water and finally dried in a nitrogen stream. As prepared samples were pressed together with a Cu-plate contact against an O-ring (1 cm^2 of Ti-surface exposed to the electrolyte) in an electrochemical cell. For anodic treatment we used a high-voltage potentiostat Jaisle IMP 88 PC – 200 V using a conventional three-electrode configuration with a platinum gauze as a counter electrode and a Haber-Luggin capillary with Ag/AgCl (1 M KCl) electrode as a reference electrode. All anodization experiments were carried out at room temperature with no stirring. The electrolytes consisted of X_2SO_4 (1 M, if not denoted otherwise) and XF (between 0.1 and 1 wt.%), where X represents; Cs^+ , K^+ , Na^+ , NH_4^+ cations. All solutions were prepared from reagent grade chemicals and DI water. The electrochemical treatment consisted of a potential ramp from the open-circuit potential (OCP) to 20 V with a different sweep rates (0.01–1 V/s) followed by holding the potential constant at 20 V for different times. After experiments the samples were rinsed with DI water and dried in a nitrogen stream.

For the structural and morphological characterization of the anodized samples, top view, cross-sectional and bottom view electron microscope (SEM) observations and direct SEM cross-sectional thickness measurements were carried out using a Hitachi FE-SEM S4800. The cross-section images were taken from mechanically bent samples, where a lift-off of the porous layer occurred. The structure of the samples was identified using X-ray diffractometer (Phillips Xpert-MPD PW3040). The composition of the porous layers was characterized by energy dispersive X-ray analyser (EDAX Genesis) fitted to the Hitachi FE-SEM S4800. Additionally, the composition of the uppermost part of the nanotubes was investigated by X-ray photoelectron spectroscopy (PHI 5600 XPS) using the Ti peak at 459 eV, the O peak at 529 eV, the F peak at 685 eV and the C peak at 285 eV.

Results and discussion

In our previous work we investigated among other parameters the influence of applied potential on the pore morphology. We have shown that best results in view of self-organization of the pores are achieved when using the applied anodic potential of 20 V. Therefore we keep this parameter identical within the frame of the different conditions used in this work.

Figure 1 shows the current transients recorded during the potentiostatic experiment at 20 V after potential ramp from the open-circuit potential (OCP) to 20 V (ramping speed

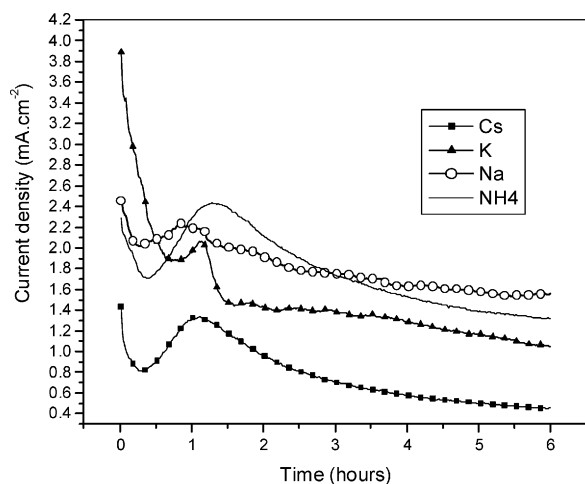


Fig. 1 Current transients recorded at 20 V after the potential ramp from OCP to 20 V (sweep rate 100 mV/s) during 6 hours of anodization in 0.2 M SO_4^{2-} /0.5 wt.% F^- electrolytes of Cs^+ & K^+ and 1 M SO_4^{2-} /0.5 wt.% F^- electrolytes of Na^+ & NH_4^+

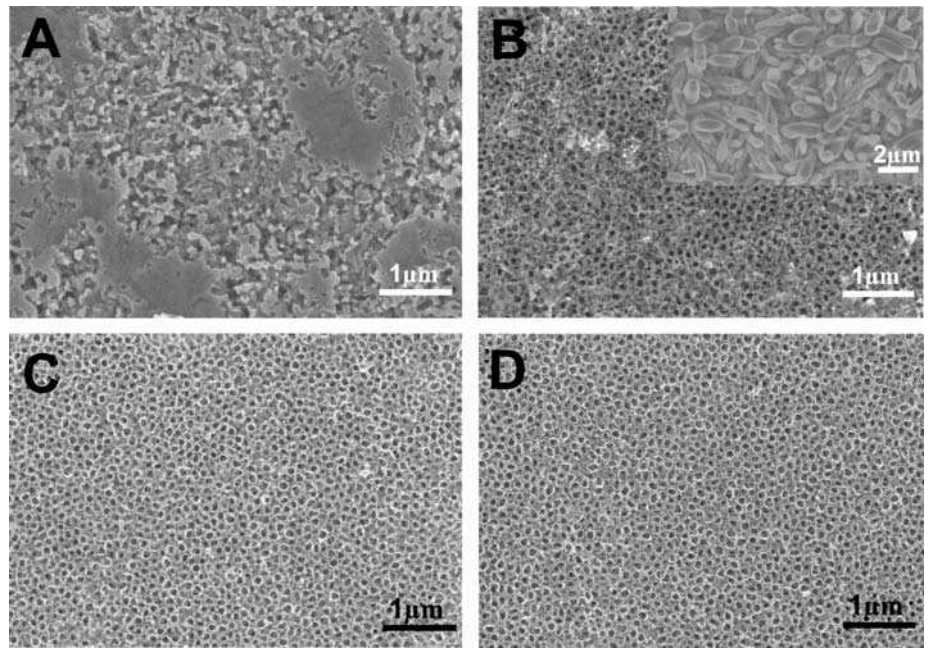
100 mV/sec) in 0.2 M SO_4^{2-} /0.5 wt.% F^- electrolytes of Cs^+ & K^+ and 1 M SO_4^{2-} /0.5 wt.% F^- electrolytes of Na^+ & NH_4^+ during 6 hours. In the first case, the lower SO_4^{2-} concentration (<1 M) is used due to a limited solubility of F^- . It is apparent from Fig. 1 that the current transients exhibit in all electrolytes very similar behaviour. During the initial current density decay, which can be ascribed to high-field TiO_2 formation represented by typical exponential current decay [38], is about 50 nm thick compact TiO_2 formed [39]. After this first step, the current density starts to raise to a certain maximum. This event can be ascribed to a random drilling of pits and worm-like pores on the oxidized surface. Afterwards the current density decays again. In line with other work [39] this is a signal that the structure becomes self-organized and reduces thereby the active area and finally, when the stable shape of the pores is established and the growth rate (as a result of dissolution and oxidation rate) of the pores is stabilized, the system reaches the steady-state [39]. From Fig. 1 it is also evident that the current densities vary with different electrolytes and also their maximum values linked to the time scale have slightly different positions. This finding reveals that samples, which are anodized in different electrolytes, need a certain time until their structures become self-organized, in other words till the anodization attains in the steady state situation. The highest current density is achieved in case of NH_4^+ -electrolytes. This is in line with previous work [19], where the highest resolution and especially the highest aspect ratio nanotubes were achieved in this electrolyte.

Figure 2 shows the SEM top-view images of the nanotube titania layers formed under conditions used in Fig. 1. Figure 2(a) shows sample after anodization in 0.2 M Cs_2SO_4 containing 0.5 wt.% CsF , which results in a non-uniform

structure, far from being organized, with some small patches of pores between large non-porous areas. Apparently, the morphology is not uniform on the entire surface in the same manner, there are areas that are preferentially etched. Figure 2(b) shows situation, which occurs when anodizing in 0.2 M K_2SO_4 solution containing 0.5 wt.% KF . In this case, the pores seem to be more organized and the structure shows some degree of homogeneity, but the pores are covered on almost all the entire area ($\sim 99\%$) with insoluble salt precipitated whiskers-like layer (see inset in Fig. 2(b)), which is most likely consisting of potassium titanates with different stoichiometry [40]. In the case of K^+ -electrolytes, several experiments have been performed with assistance of a thermostat at elevated temperatures ($\sim 70^\circ\text{C}$), what could actually allow us to use higher concentration of sulphates due to higher solubility, but the degree of precipitation was nearly the same. Different situations were observed when samples were anodized in solutions of Na^+ or NH_4^+ . Figures 2(c) and (d) show the porous structures formed by anodization in 1 M Na_2SO_4 + 0.5 wt.% NaF , resp. 1 M $(\text{NH}_4)_2\text{SO}_4$ + 0.5 wt. NH_4F % solutions, which result in far more homogenous nanotubular structures. The inner nanotube diameter is approximately 100 nm, the spacing between the nanotubes is about 150 nm in average and the wall thickness is about 15 nm. By using last two electrolytes, the surfaces of the nanotube layers after several hours of the anodization experiment are uniform and regular, without any significant remains of precipitates.

Figure 3 shows cross-section images of self-organized nanotubes formed as in Fig. 1. The first two images reveal that the self-organized nanotube formation in Cs^+ (Fig. 3(a)) or K^+ (Fig. 3(b)) electrolyte is strongly influenced by precipitation of insoluble species as shown in Fig. 2(a) and (b). It can be clearly seen that the nanotubes are covered with layer of precipitates, which hinders the flux of ions to be continuous and uniformly distributed. Therefore the final resolution of the anodization process is very low. The achieved lengths of the nanotube layers is in range of several hundreds of nm (~ 500 nm). When anodizing in Na^+ (Fig. 3(c)) or NH_4^+ -electrolytes (Fig. 3(d)), the resulting structure consists of self-organized high aspect ratio vertically standing and well adhered nanotube layers on the Ti substrate. They are present without any significant covering particles, if the anodization time is sufficiently long (minimal 2 hours and more). As polarization time vs. SEM characterizations revealed, the initial compact TiO_2 layer formed in the first stage (see Fig. 1) can be found on the surface to some extent within first dozens of minutes, but then as the uppermost part of the tubes is being dissolved during the anodization (the dissolution rate on the pore tip is smaller than on the pore bottom, but not negligible), this oxide layer is dissolved as well. As we already reported, so far is the maximum achieved lengths of the nanotubes formed in sulphate-based electrolytes $2.4\text{ }\mu\text{m}$ with NaF addition [18] and $2.5\text{ }\mu\text{m}$ with NH_4F addition [19]. From Figs. 2

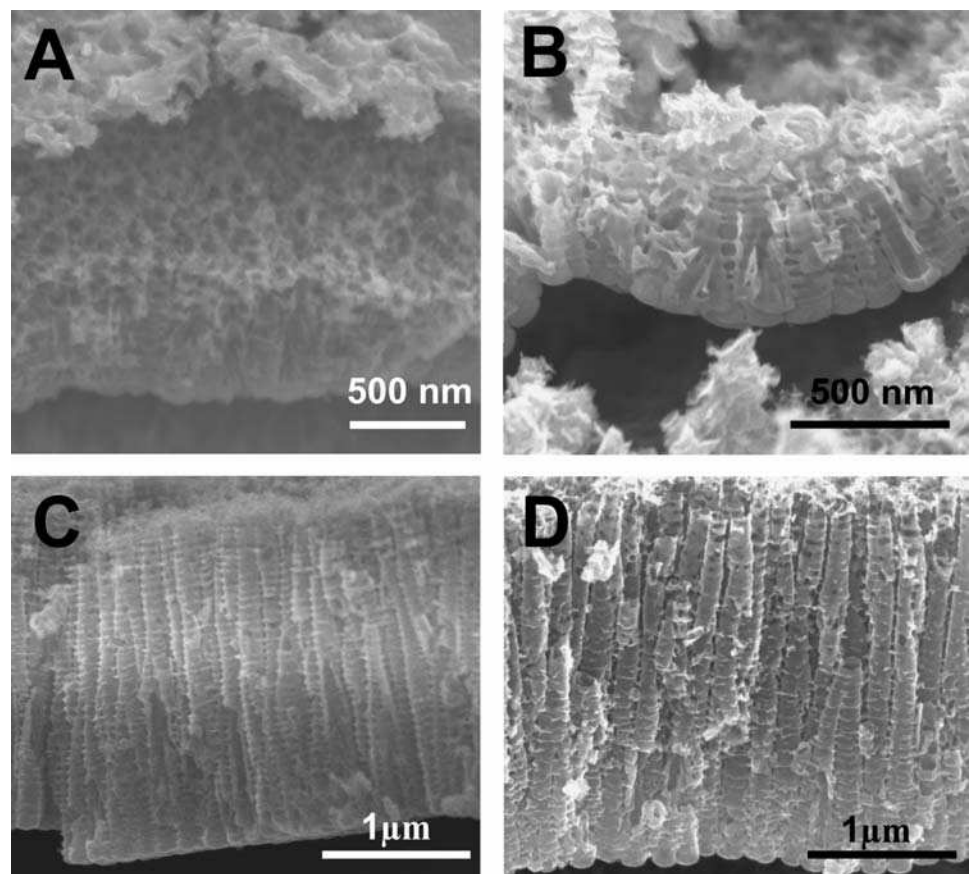
Fig. 2 SEM top-view images of samples formed as in Fig. 1. (A) represents the sample anodized in Cs^+ electrolyte; (B) in K^+ ; (C) in Na^+ and (D) in NH_4^+ . The inset in B shows precipitates of potassium titanates on the surface



and 3 arise that to form high-aspect ratio self-organized TiO_2 nanotubes in a uniform and homogenous manner, Na^+ —or NH_4^+ —electrolytes can be used rather than Cs^+ or K^+ —the latter lead to irregularities and precipitation of salt layers.

Figure 4 shows the XRD patterns of samples before (Fig. 4(a)) and after annealing (Fig. 4(b)) in air at 450°C for 3 hours with heating and cooling rate $30^\circ\text{C}/\text{min}$. The sample was anodized for 6 hours in 1 M $(\text{NH}_4)_2\text{SO}_4 + 0.5 \text{ wt. } \text{NH}_4\text{F}$

Fig. 3 SEM cross-section images of samples formed as in Fig. 1. (A) represents the sample anodized in Cs^+ electrolyte; (B) in K^+ ; (C) in Na^+ and (D) in NH_4^+ . The cross-sections were taken from mechanically cracked samples



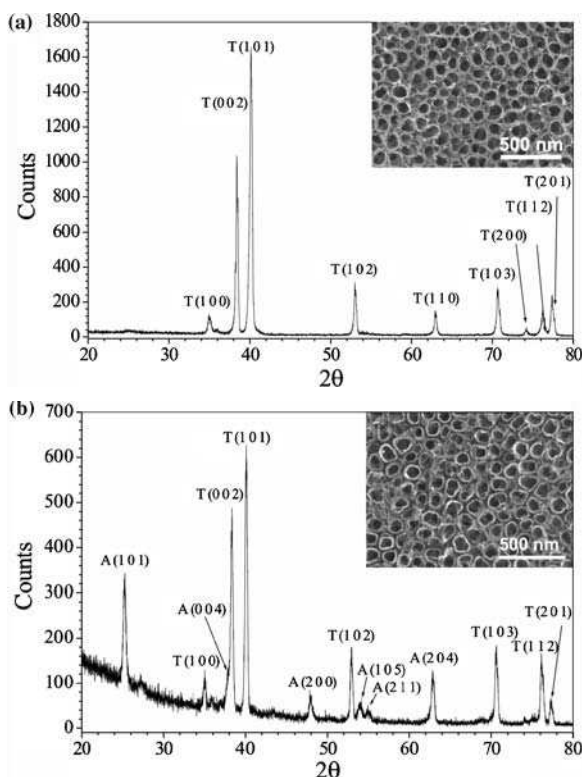


Fig. 4 XRD patterns of TiO_2 before and after annealing in air at 450°C for 3 hours with heating and cooling rate $30^\circ\text{C}/\text{min}$. The presence of anatase phase after annealing is observed. The sample was anodized as in Fig. 1 in NH_4^+ electrolyte. The SEM top-view insets shows surface of the nanotubes before and after annealing

% electrolyte at 20 V. In general, the XRD measurements of all as-anodized samples reveal that the self-organized TiO_2 nanotubes have amorphous structure. This is in line with Fig. 4(a), where only Ti-peaks are recorded, because the X-ray reveals also the Ti-substrate information even when a very low X-ray angle is used ($<1^\circ$). The phase transformation from amorphous phase to anatase or rutile crystalline phase can be achieved for instance upon annealing—this is in line with some previous annealing experiments on porous TiO_2 [41]. Figure 4(b) shows clearly anatase peaks and again Ti-peaks from the substrate are present. The inset pictures in Fig. 4(a) and (b) compare the top-view of the nanotubes before and after annealing and claim that their morphology during the annealing remains unchanged.

The composition of the nanotube layers was determined by XPS and EDX. Figure 5(A) shows XPS spectra of the nanotube layer surface formed in NH_4^+ electrolyte. Figure 5(B) shows EDX spectra of the composition of the same sample through the nanotube layer. The inset in Fig. 5(b) shows an average values of all elements in atomic and weight %. Evidently, the nanotubes are consisting of TiO_2 . Sulphates from the electrolytes are not detected in any case, while some

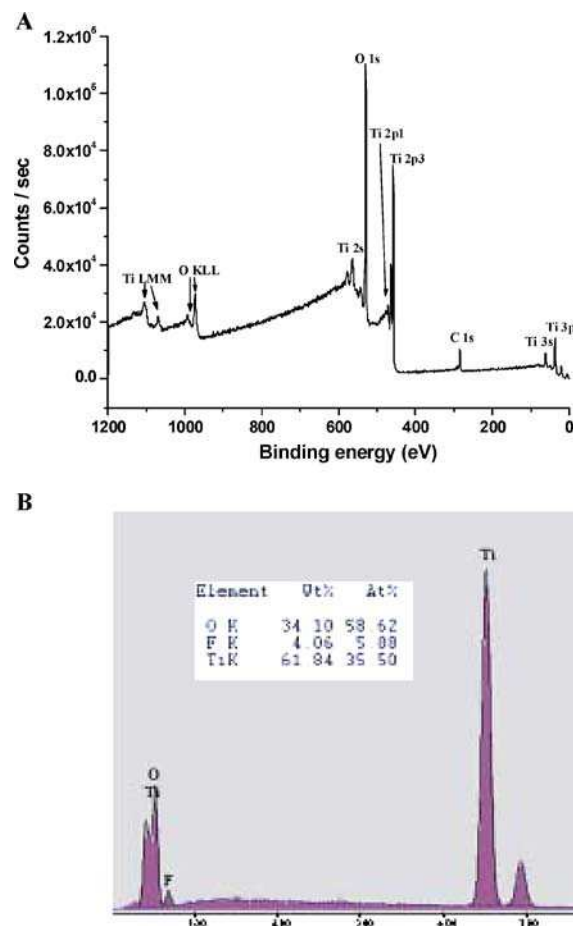


Fig. 5 The XPS survey (A) and the EDX spectra (B) of the nanotube layer surface formed in the NH_4^+ electrolyte, showing the composition of the nanotubes of the same sample. The inset shows an average values of all elements detected over the layer in atomic and wt %

traces of fluorides are detected through the layer, but in an almost negligible amount.

Conclusions

We have investigated the formation of self-organized TiO_2 nanotube layers in sulphate electrolytes containing small amounts of different fluorides. In case of $\text{Cs}_2\text{SO}_4/\text{CsF}$ and $\text{K}_2\text{SO}_4/\text{KF}$ electrolytes the uniformity of the nanotubular layers is low, in particular because of high degree of precipitation and non-uniform TiO_2 dissolution. For this reason their usage seem to be not suitable. Furthermore, the presented results show and confirm that by using $\text{Na}_2\text{SO}_4/\text{NaF}$, resp. $(\text{NH}_4)_2\text{SO}_4/\text{NH}_4\text{F}$ electrolytes, a high resolution nanotube layers can be achieved. In these electrolytes the nanotube layers can be grown to a thickness of approximately 2.4, resp. 2.5 μm under optimized conditions that

are anodic potential, fluoride content and polarization time. The self-organized nanotube layers are consisting of TiO₂ in amorphous phase, which can be transformed to anatase upon annealing. Such a heat treatment does not change either the pore morphology nor the thickness of the layers. Some negligible traces of fluorides from the electrolytes are detected in the nanotube layers, sulphates are not detected in any case. Present results show various experimental means to cover titanium surface by highly organized high-aspect ratio titania nanotubes, which offer several potential applications, by a quick and low-cost electrochemical approach.

Acknowledgments The authors thank the Socrates/Erasmus Program between ICT Prague and FAU Erlangen for financial support of K. Sirotna, A. Friedrich, H. Hildebrand and U. Marten-Jahns are acknowledged for SEM, XPS and XRD investigations.

References

1. H. Masuda and K. Fukuda, *Science*, **268**, 1466 (1995).
2. O. Jessensky, F. Muller, and U. Gösele, *Appl. Phys. Lett.*, **72**, 1173 (1998).
3. L.T. Canham, *Appl. Phys. Lett.*, **57**, 1046 (1990).
4. V. Lehman and H. Föll, *J. Electrochem. Soc.*, **137**, 653 (1990).
5. H. Tsuchiya, M. Hueppe, T. Djenizian, and P. Schmuki, *Surf. Sci.*, **547**, 268 (2003).
6. H. Masuda and K. Fukuda, *Appl. Phys. Letters*, **78**, 826 (2001).
7. H. Masuda, M. Ohya, H. Asoh, M. Nakao, M. Nohtomi, and T. Tamamura, *Jpn. J. Appl. Phys.*, **38**, L1403 (1999).
8. R.B. Wehrspohn, K. Nielsch, A. Birner, J. Schilling, F. Müller, A.P. Li, and U. Gösele, *Pits and Pores II*, edited by P. Schmuki, D.J. Lockwood, Y.H. Ogata, and H.S. Isaacs, Proc. Vol. ECS 2000-25 (2000) p. 168.
9. V. Zwillling, M. Aucouturier, and E. Darque-Ceretti, *Electrochim. Acta*, **45**, 921 (1999).
10. M. Gotic, M. Ivanda, A. Sekulic, S. Music, S. Popovic, A. Turkovic, and K. Furic, *Mater. Lett.*, **28**, 225 (1996).
11. Li, W., Shah, S. I., C.-P. Haung, and C. Ni, *Mater. Sci. Eng. B*, **96**, 247 (2002).
12. J. Choi, R.B. Wehrspohn, J. Lee, and U. Gösele, *Electrochim. Acta*, **49**, 2645 (2004).
13. Y.T. Sul, C.B. Johansson, S. Petronis, A. Krozer, Y. Jeong, A. Wennerberg, and T. Albrektsson, *Biomaterials*, **23**, 491 (2002).
14. J.C. Marchenoir, J.P. Loup, and J. Masson, *Thin Solid Films*, **66**, 357 (1980).
15. Y. Mueller and S. Virtanen, *Pits and Pores II*, edited by P. Schmuki, D.J. Lockwood, Y.H. Ogata, and H.S. Isaacs, Proc. Vol. ECS 2000-25 (2000) p. 294.
16. D. Gong, C.A. Grimes, O.K. Varghese, W. Hu, R.S. Singh, Z. Chen, and E.C. Dickey, *J. Mater. Res.*, **16**, 3331 (2001).
17. R. Beranek, H. Hildebrand, and P. Schmuki, *Electrochem. Solid-State Lett.*, **6**, B12 (2003).
18. J.M. Macak, K. Sirotna, and P. Schmuki, *Electrochim. Acta*, **50**, 3679 (2005).
19. J.M. Macak, H. Tsuchiya, and P. Schmuki, *Angew. Chem. Int. Ed.*, **44**, 2100 (2005).
20. A. Ghicov, H. Tsuchiya, J.M. Macak, and P. Schmuki, *Electrochem. Commun.*, **7**, 505 (2005).
21. K.S. Raja, M. Misra, and K. Paramguru, *Electrochim. Acta*, **51**, 154 (2005).
22. J. Zhao, X. Wang, R. Chen, and L. Li, *Solid St. Comm.*, **134**, 705 (2005).
23. X. Quan, S. Yang, X. Ruan, and H. Zhao, *Environ. Sci. Technol.*, **39**, 3770 (2005).
24. Q. Cai, M. Paulose, O.K. Varghese, and C.A. Grimes, *J. Mat. Res.*, **20**, 230 (2005).
25. A. Fujishima, T.N. Rao, and D.A. Tryk, *J. Photochem. Photobiol. C-Photochem. Rev.*, **1**, 1 (2001).
26. O.K. Varghese, D. Gong, K.G. Ong, and C.A. Grimes, *Sensors and Actuators*, **B93**, 338 (2003).
27. D.M. Brunette, P. Tengvall, M. Textor, and P. Thomsen, *Titanium in Medicine* (Springer, Berlin, 2001).
28. J.M. Macak, H. Tsuchiya, L. Taveira, and A. Ghicov, *J. Biomed. Mat. Res.*, in press.
29. H. Tsuchiya and P. Schmuki, *Electrochem. Commun.*, **6**, 1131 (2004).
30. H. Tsuchiya, J.M. Macak, L.V. Taveira, and P. Schmuki, *Chem. Phys. Lett.*, **410**, 188 (2005).
31. H. Tsuchiya and P. Schmuki, *Electrochem. Commun.*, **7**, 49 (2005).
32. H. Tsuchiya, J.M. Macak, I. Sieber, L. Taveira, A. Ghicov, K. Sirotna, and P. Schmuki, *Electrochem. Commun.*, **7**, 295 (2005).
33. I. Sieber, B. Kannan, and P. Schmuki, *Electrochem. Solid-State Lett.*, **8**, J10 (2005).
34. I. Sieber and P. Schmuki, *J. Electrochem. Soc.*, in press.
35. I. Sieber, H. Hildebrand, A. Friedrich, and P. Schmuki, *Electrochem. Commun.*, **7**, 97 (2005).
36. N.T.C. Oliveira, S.R. Biaggio, R.C. Rocha-Filho, and N. Bocchi, *J. Braz. Chem. Soc.*, **13**, 463 (2002).
37. H. Tsuchiya, J.M. Macak, I. Sieber, and P. Schmuki, *Small*, **1**, 722 (2005).
38. J.W. Schultze, M.M. Lohrengel, and D. Ross, *Electrochim. Acta*, **28**, 973 (1983).
39. L. Taveira, J.M. Macak, H. Tsuchiya, L.F.P. Dick, and P. Schmuki, *J. Electrochem. Soc.*, **152**, B405 (2005).
40. N. Bao, X. Feng, X. Lu, and Z. Yang, *J. Mater. Sci.*, **37**, 3035 (2002).
41. O.K. Varghese, D. Dong, M. Paulose, C.A. Grimes, and E.C. Dickey, *J. Mater. Res.*, **18**, 156 (2003).